ICM11

Stress Corrosion Cracking of Novel Steel for Automotive Applications

Muhammed. Khalissi[a], R.K. Singh Raman[a,b], S. Khoddam[a],[a]*

[a]Department of Mechanical and Aerospace Engineering, Monash University, Melbourne, Victoria 3800, Australia
[b]Department of ChemicalEngineering,MonashUniversity,Melbourne,Victoria3800, Australia

Abstract

In the present study, susceptibility of a high manganese TWIP steel to stress corrosion cracking (SCC) in a 3.5% NaCl solution was investigated using slow strain rate tests (SSRT), constant load (CL) tests and fractography. Strain rates employed for SSRT were in the range of 10^{-06} - 10^{-08} s^{-1}. The specimens tested in air revealed a ductile type of failure, whereas those tested in the corrosive solution exhibited a brittle feature that is attributed to stress corrosion cracking. SCC was observed at a relatively low strain rate of $10^{-07} s^{-1}$.

Selection and/or peer review under responsibility of [name organizer]
Keywords: TWIP steels; Strain rate; SSRT; SCC; Constant load test; CL; NaCl solution; Twinning.

1. Introduction

High manganese (20-30 wt.%) TWIP steels offer enormous potential in applications for structural components for the automotives, due to their exceptional combination of tensile strength and ductility. These steels might also be considered as an alternative to common austenitic Cr-Ni stainless steels [1, 2]. To initiate twinning, the material must possess a relatively low level of the stacking fault energy. In high manganese steels (e.g., Fe-25Mn-3Si-3Al alloy), the stacking fault energy is so low (SFE $\leq$ 20 mJ/m^2) that twinning commences early, and the steel starts to deform at around 300 MPa. This phenomenon is referred to as "Twinning Induced Plasticity" [3].

Stress corrosion cracking (SCC) is a crucial mode of failure which has to be considered before any new class of materials can be utilized in corrosive environment (such as polluted industrial environments,

---

* Muhammed, Khalissi. Tel.: +61 3 9905 9595; fax: +61 3 9905 9628.
E-mail address: Muhammed.Khalissi@eng.monash.edu.au.

marine condition or for automotive components). Though there are reports on electrochemical corrosion of TWIP steels [4-6], SCC properties of these steels have received little attention.

This paper presents investigation on the SCC susceptibility of a high–Mn TWIP steel at different strain rates as well as under constant load.

2. Experimental

The chemical composition of the high-manganese austenitic TWIP steel used in this study is shown in Table 1.

Table 1. Chemical analysis of the TWIP-steel (wt %)

C	Si	Mn	P	S	Cr	Mo
0.018	3.56	26.34	0.009	0.04	0.062	0.002
Ni	Al	Co	Cu	Nb	Ti	V
0.035	4.84	0.005	0.078	0.04	0.004	0.032
W	Pb	N	Fe			
0.007	0.284	0.0133	64.2			

The steel was received as an ingot of 200×140×40 mm. This ingot was subjected to thermo-mechanical processing, which included hot rolling, cold rolling and heat treatments.

Slow strain rate tests (SSRT) were carried out on smooth cylindrical specimens (the total length (L) = 200 mm, diameter (d) = 8 mm, gauge diameter (d_o) = 3 mm, and gauge length of (L_o) = 20 mm). SCC susceptibility was estimated by using of the range of strain- rates (1×10^{-06} to 2×10^{-08} s^{-1}), which is consistent with the guidelines in MTI publication no. 15 [7].

The test solutions used was 3.5 % NaCl (pH = 6.24). All experiments were carried out under an open circuit condition. The TWIP samples and rigs used in constant load tests were similar to those used for SSRT. The samples were loaded at different constant initial stresses (σ_o) in the range 315 - 460 MPa.

Fracture surface was cleaned to remove the corrosion products and the fracture features were examined using scanning electron microscope of the JEOL 840A.

3. Results and Discussion

3.1. SSRT and Index of Susceptibility

Strain rate is reported to have a profound influence on whether or not an alloy will undergo SCC [8, 9]. Stress-strain curves in Figure 1(a) show that not only is the ultimate tensile strengths dependent upon the presence or otherwise of stress corrosion cracks, but so also is the total elongations achieved [10].

Index of susceptibility is a practical indication for evaluation of stress corrosion cracking, which is defined as "an average percentage of decrease in the values measured when examining parameter values obtained in a corrosive environment, and compared to those obtained in air" [11-13].

Table 2 shows different indices of susceptibility of TWIP steel. For example, I_{tf} is the ratio of time to failure in chloride solution and air. Other indices represent similar ratios on the basis of reduction of area (I_A), strain energy (I_E), maximum stress (I_R) and plastic elongation (I_Z). The closer the index value to 100, the greater is susceptibility to SCC. Figure 1(b) shows the effect of strain rate on reduction of area and time to failure in 3.5% NaCl solution. The data in Table 2 suggests a great susceptibility of SCC at the

low strain rate (4×10^{-07} s^{-1}). The high strain rates allow less time for corrosive action and therefore, the lesser propensity for SCC. Fractographic features may provide distinctive feature for SCC.
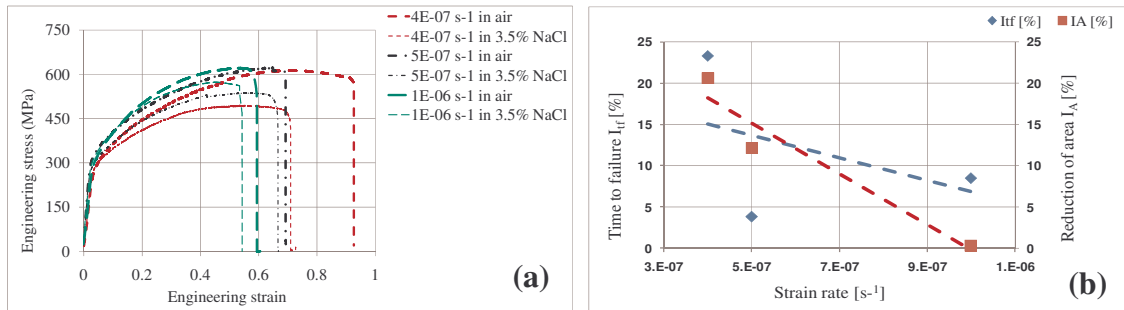

Fig. 1. (a) Engineering stress-strain curves for TWIP steel tested at room temperature and different strain rates in air and 3.5 % NaCl solution; (b) Susceptibility indices of TWIP steels show the effect of strain rates on the time to failure (I_{tf}) and reduction of area (I_A) in 3.5% NaCl solution.

Table 2. Susceptibility indices of TWIP steel at different strain rates.

Strain rate [s^{-1}]	Max. stress (I_R) [%]	Strain energy (I_E) [%]	Time to failure (I_{tf}) [%]	Reduction of area (I_A) [%]	Plastic elongation (I_Z) [%]
4×10^{-07}	22	37	23	21	24
5×10^{-07}	19	12	4	12	5
1×10^{-06}	13	13	8	0.3	5

The pertinent fractographic features for SCC are: intergranular and/or transgranular cracking [14], and the evidence of secondary cracking [15]. Such features were either considerably less prominent or absent in the case of specimens tested at high strain rates, as shown in figure 2(a) and 2(b). The predominant feature of ductile dimples in these specimens is similar to that observed in the specimens tested at all strain rates in air (Figure 2(c)). On the other hand, a considerable fraction of the fracture surface of the specimen tested in sodium chloride at a lower strain rate (4×10^{-07} s^{-1}) clearly possessed transgranular and intergranular cracking (Figure 3(a)) and secondary cracking (Figure 3(b)). However, the transgranular cracking clearly predominates intergranular cracking.
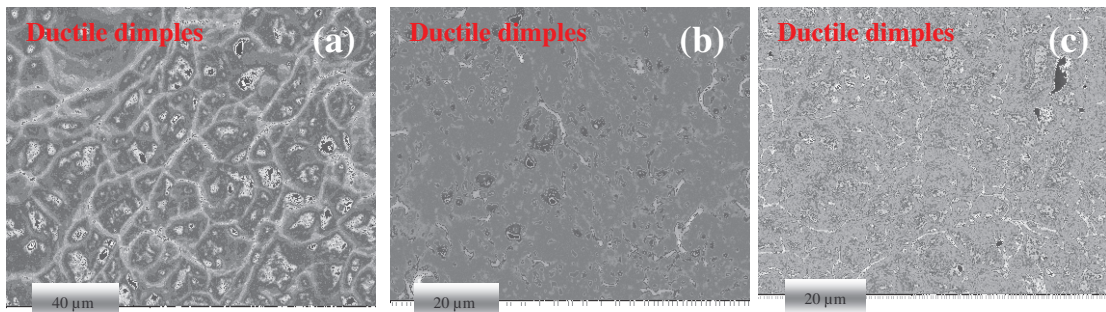

Fig. 2. SEM fractographs of TWIP steel showing: (a) ductile fracture at 5×10^{-07}s^{-1} strain rate in 3.5% NaCl solution; (b) ductile fracture at 1×10^{-06} s^{-1} strain rate in 3.5% NaCl solution; (c) representative fractograph showing ductile dimples in specimen tested at 4×10^{-07} s^{-1} strain rate in air.
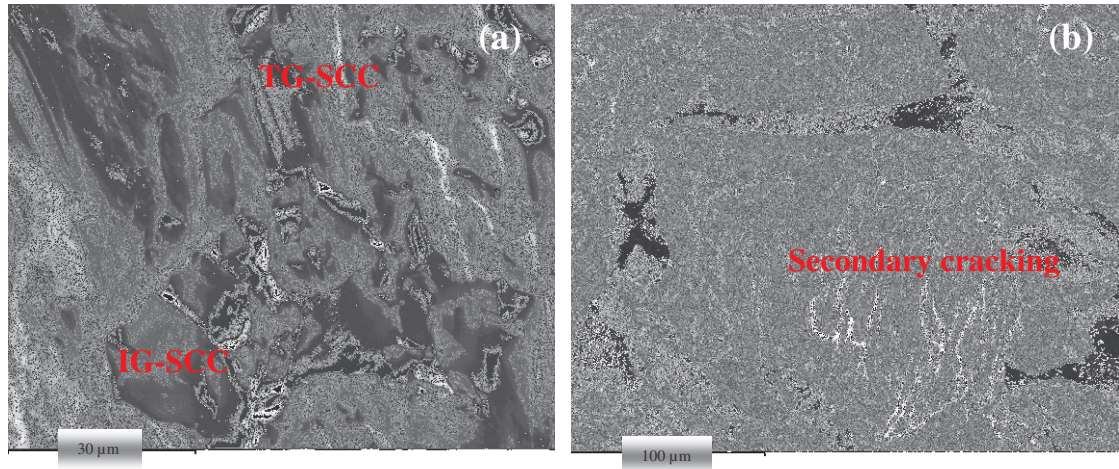
Fig. 3. SEM fractographs of TWIP steel after SSRT at 4×10^{-07} s^{-1} strain rate in 3.5% NaCl solution showing: (a) transgranular and intergranular cracking over fracture surface and; (b) secondary cracking in the gauge section.

Though the SSRT results and fractographic evidence have established SCC of the TWIP steel in 3.5% chloride sodium, it is still unclear whether greater propensity of the new twin that may form during the dynamic loading in SSRT could play a role. Therefore, a few tests were also conducted under static loading condition.

3.2. Constant Load tests

The constant load (CL) tests in 3.5% NaCl solutions were conducted at 315 MPa i.e., (below the yield strength), 380 MPa and 460 MPa i.e., (above the yield strength but below UTS). These tested were terminated at 1120h. Gauge length section of the specimens was examined by SEM for investigative the presence of secondary cracking. Then the specimens were strained further in air at a high strain rate (1×10^{-06} s^{-1}) until they fractured.

SEM photographs in Figure 4(a-d) illustrate the change in the features along the gauge length of the specimen, from the quasi cleavages at low stresses (below yield stress) to transgranular SCC (above the yield stress) and/or to the intergranular SCC at a considerably high stress.

Presence of inter- or transgranular features in gauge length sections confirm that TWIP steel had undergone stress corrosion cracking.
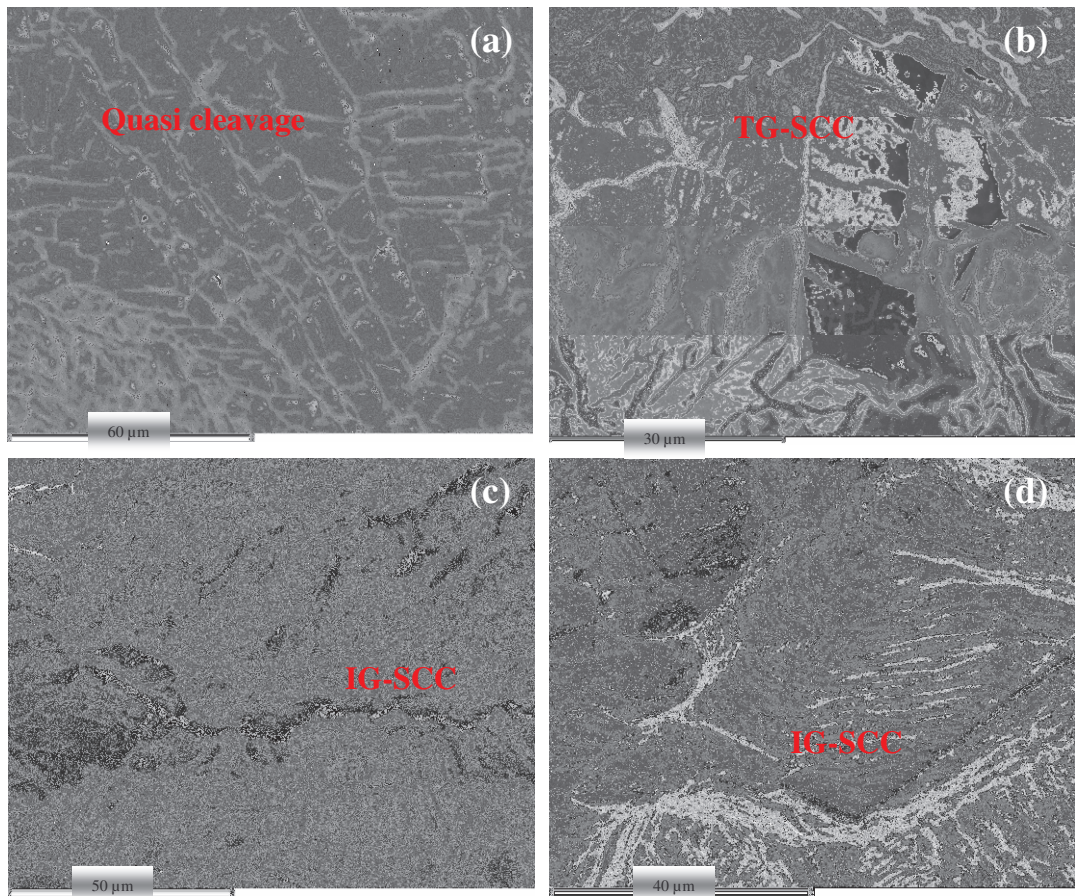
Fig. 4. SEM photographs showing SCC features along the gauge length of the specimen after 1120h at 3.5% NaCl solution in CL tests: (a) quasi cleavage at the applied stress below the yield strength, (b) transgranular SCC at the applied stress above the yield strength, (c and d) intergranular SCC at the applied stress below the UTS.

4. Conclusion

- SSRT of the TWIP steel in 3.5% NaCl resulted in SCC at a strain rate of $10^{-07}\,s^{-1}$, whereas the higher strain rates produced exclusive mechanical fracture.
- Constant load tests have confirmed the results of SSRT, and showed that the features of SCC change with increasing constant initial load.

Acknowledgment

References

[1]   Chang SC, Liu JY, Juang HK. Environment-Assisted Cracking of Fe-32% Mn-9% Al Alloys in 3.5% Sodium Chloride Solution. Corrosion, vol. 51, 1995.

[2]   Tjong SC. Stress corrosion cracking of the austenitic Fe-Al-Mn alloy in chloride environment. Materials and Corrosion/Werkstoffe und Korrosion 1986;37.

[3]   Schroder T. cooking steel for the cars of tomorrow. Max Planck Research 2004.

[4]   Hamada AS, Karjalainen LP, El-Zeky MA, Philippe M, Vincent M. Effect of anodic passivation on the corrosion behaviour of Fe-Mn-Al steels in 3.5%NaCl. Amsterdam: Elsevier Science, 2006. p.77.

[5]   Zhang YS, Zhu XM, Zhong SH. Effect of alloying elements on the electrochemical polarization behavior and passive film of Fe-Mn base alloys in various aqueous solutions. Corrosion Science 2004;46:853.

[6]   Kannan MB, Raman RKS, Khoddam S. Comparative studies on the corrosion properties of a Fe-Mn-Al-Si steel and an interstitial-free steel. Corrosion Science 2008;50:2879.

[7]   Beavers JA, Koch GH, Materials Technology Institute of the Chemical Process I. Limitations of the slow strain rate test for stress corrosion cracking testing. Corrosion(USA) 1991;48:256.

[8]   Maiya PS. Prediction of environmental and strain-rate effects on the stress corrosion cracking of austenitic stainless steels. United States, 1985. p.Size: Pages: 32.

[9]   Singh Raman RK. Evaluation of caustic embrittlement susceptibility of steels by slow strain rate testing. Metallurgical and Materials Transactions A 2005;36:1817.

[10]   Parkins RN. Stress Corrosion Cracking-The Slow Strain Rate Technique. ASTM STP 1979;665:5.

[11]   Sieradzki K. Stress corrosion cracking. Technical brief 2003.

[12]   Specimens SCT. Standard Practice for Slow Strain Rate Testing to Evaluate the Susceptibility of Metallic Materials to Environmentally Assisted Cracking1.

[13]   Czechowski M. Slow-strain-rate stress corrosion testing of welded joints of Al-Mg alloys. Achievements in Materials and Manufacturing Engineering 2007;20:219.

[14]   Pal S, Singh Raman RK. Determination of threshold stress intensity factor for stress corrosion cracking (KISCC) of steel heat affected zone. Corrosion Science 2009;51:2443.

[15]   Asphahani AI. Slow Strain-Rate Technique and Its Applications to the Environmental Stress Cracking of Nickel-Base and Cobalt-Base Alloys. Stress corrosion cracking: the slow strain-rate technique 1979:279.